

# Nanoscale

Accepted Manuscript



This is an *Accepted Manuscript*, which has been through the Royal Society of Chemistry peer review process and has been accepted for publication.

*Accepted Manuscripts* are published online shortly after acceptance, before technical editing, formatting and proof reading. Using this free service, authors can make their results available to the community, in citable form, before we publish the edited article. We will replace this *Accepted Manuscript* with the edited and formatted *Advance Article* as soon as it is available.

You can find more information about *Accepted Manuscripts* in the [Information for Authors](#).

Please note that technical editing may introduce minor changes to the text and/or graphics, which may alter content. The journal's standard [Terms & Conditions](#) and the [Ethical guidelines](#) still apply. In no event shall the Royal Society of Chemistry be held responsible for any errors or omissions in this *Accepted Manuscript* or any consequences arising from the use of any information it contains.



Eco-materials and Renewable Energy Research Center (ERERC)  
National Laboratory of Solid State Microstructures  
Nanjing University

---

Tangzhong Ying Building C412, Nanjing University, 22 Hankou Road, Nanjing, Jiangsu 210093, P. R. China: +86-25-8362-1372 E-mail: zhouyong1999@nju.edu.cn

18-Dec-2015

Dr. Shouheng Sun  
Associate Editor, Nanoscale

**Re: Manuscript ID: NR-ART-10-2015-007376**

Dear Editor Shouheng Sun,

Thank you very much for your e-mail of 12-Dec-2015, with regard to our manuscript (**Manuscript ID: NR-ART-10-2015-007376**) entitled “In Situ Direct Growth of Single Crystalline Metal (Co, Ni) Selenium Nanosheets on Metal Fibers as Counter Electrodes toward Low-cost, High-Performance Fiber-shaped Dye-sensitized Solar Cells”, together with the comments from reviewer. We appreciate additional and very valuable comments from the reviewers. We are also glad to learn that our manuscript may become acceptable for publication in *Nanoscale*.

I am sending here with our revised manuscript in response to the comments and suggestions. We have made the changes as marked with red color in the revision. Our responses to the Reviewers’ comment are summarized in the separate sheets attached.

I hope this revised manuscript would be satisfactorily improved and can be accepted for publication. We are looking forward to receiving a favorable response from your regarding our manuscript.

Very sincerely yours,

Prof. Yong Zhou

Our responses to your and the referees' comments are as follows:

**1. How about the catalytic stability of Co<sub>0.85</sub>Se and Ni<sub>0.85</sub>Se counter electrode?**

Both Co<sub>0.85</sub>Se and Ni<sub>0.85</sub>Se counter electrodes were measured 100 consecutive cyclic voltammograms (CVs). The resulting CV curves have almost no change, indicating that the two electrodes are of high stability.

**2. Why did the Ni<sub>0.85</sub>Se-based FDSSC achieve higher power conversion efficiency than the Co<sub>0.85</sub>Se-based one?**

The Ni<sub>0.85</sub>Se electrode has better electrocatalytic active than Co<sub>0.85</sub>Se electrode, which was confirmed by the smaller charge-transfer resistance ( $R_{ct}$ ) of Ni<sub>0.85</sub>Se electrode.

**3. What is the reason that the  $Z_N$  of Pt electrode is smaller than the resultants of Co<sub>0.85</sub>Se and Ni<sub>0.85</sub>Se?**

Co<sub>0.85</sub>Se and Ni<sub>0.85</sub>Se counter electrodes have electrocatalytic active films with several micrometers thickness, which increased the resistance of I<sub>3</sub><sup>-</sup>/I<sup>-</sup> ion diffusion. However, for Pt counter electrode, the I<sub>3</sub><sup>-</sup> reduction reaction just occurs on its smooth surface.

# *In Situ* Direct Growth of Single Crystalline Metal (Co, Ni) Selenium Nanosheets on Metal Fibers as Counter Electrodes toward Low-cost, High-Performance Fiber-shaped Dye-sensitized Solar Cells

Liang Chen<sup>†a</sup>, Hexing Yin<sup>†b</sup>, Yong Zhou<sup>a, c\*</sup>, Hui Dai<sup>a, d</sup>, Tao Yu<sup>a, c</sup>, Jianguo Liu<sup>a, c</sup> and Zhigang Zou<sup>a, c\*</sup>

Received (in XXX, XXX) Xth XXXXXXXXX 200X, Accepted Xth XXXXXXXXX 200X

First published on the web Xth XXXXXXXXX 200X

DOI: 10.1039/b000000x

Highly crystalline metal (Co, Ni) selenium ( $\text{Co}_{0.85}\text{Se}$  or  $\text{Ni}_{0.85}\text{Se}$ ) nanosheets were *in situ* grown on metal (Co, Ni) fibers ( $\text{M-M}_{0.85}\text{Se}$ ). Both  $\text{M-M}_{0.85}\text{Se}$  ( $\text{Co-Co}_{0.85}\text{Se}$  and  $\text{Ni-Ni}_{0.85}\text{Se}$ ) fibers prove to function as excellent, low-cost counter electrodes (CEs) in fiber-shaped dye-sensitized solar cells (FDSSCs) with high power conversion efficiency ( $\text{Co-Co}_{0.85}\text{Se}$  6.55% and  $\text{Ni-Ni}_{0.85}\text{Se}$  7.07%), comparable or even superior to Pt fiber CE (6.54%). The good performance of the present Pt-free CE-based solar cell was believed to originate from: (1) the intrinsic electrocatalytic property of the single-crystalline  $\text{M-M}_{0.85}\text{Se}$ ; (2) the enough void space among  $\text{M}_{0.85}\text{Se}$  nanosheets allows the redox ions easier diffusion; (3) the two-dimensional morphology provides the large contact area between the CE catalytic material and electrolyte; (4) *in situ* direct growth of the  $\text{M}_{0.85}\text{Se}$  on metal fiber renders the good electrical contact between the active material and the electrons collector.

## Introduction

As portable electric devices become more and more popularity, wearable devices (solar cells<sup>1</sup>, supercapacitors<sup>2</sup>, and generators<sup>3</sup>) have been rapidly attracting attentions. Fiber-shaped solar cells can be woven into wearable energy cloths (such as coats, hats or bags) to charge portable electric devices in a very handy way<sup>4</sup>. Currently, fiber-shaped dye-sensitized solar cells (FDSSCs), in sharp contrast with the flat counterpart, represent typical fiber-configuration electronics for solar energy harvesting<sup>5-13</sup>. A typical FDSSC consists of a fiber-shaped photoanode (n-type semiconductor film sensitized with dye), a redox electrolyte (an organic liquid solvent dissolving with  $\text{I}_3^-/\text{I}^-$  redox species), and a fiber-shaped counter electrode (CE).

Optimization of the  $\text{I}_3^-$  reduction reaction conducted with CE is of utmost significance for enhancement of photovoltaic performance of a FDSSC. Pt fiber proves to be a well stable and high efficient electrocatalyst in liquid state FDSSCs for  $\text{I}_3^-/\text{I}^-$  redox couple. Motivated by practical and economical considerations, great effort was made to explore low-cost, Pt-free

CE, such as specific transition metal carbides<sup>14</sup>, nitrides<sup>14, 15</sup> and chalcogens<sup>16-24</sup>. The Pt-free CE used for the FDSSC generally grows on a tread-like conductive substrate that collects electrons from the external load and transfers electrons into the electrocatalyst film<sup>13-24</sup>. The good performance of the Pt-free CE could be achieved through mediating the feature of the CE, including improving surface area, enhancing electrical conductivity, or exposing high-activity crystal facet.

In this paper, we directly grew single-crystalline metal (Ni, Co) selenium nanosheets on metal fiber (briefly called as  $\text{M-M}_{0.85}\text{Se}$ ) toward low-cost, high-performance FDSSCs. The growing  $\text{M}_{0.85}\text{Se}$  nanosheets layer acts as electrocatalytic centers for the reduction of  $\text{I}_3^-$ , and the underlying metal fiber as conductive collector for collecting electrons. Photovoltaic measurement demonstrates that the  $\text{M-M}_{0.85}\text{Se}$  thus obtained show good electrocatalytic behavior as CEs for the high-efficiency FDSSC ( $\text{Ni-Ni}_{0.85}\text{Se}$  for 7.07% and  $\text{Co-Co}_{0.85}\text{Se}$  for 6.55%), comparable or even superior to Pt fiber (6.54%). The good performance of the present Pt-free CE-based solar cell was believed to originate from: (1) the intrinsic electrocatalytic property of the single-crystalline  $\text{M-M}_{0.85}\text{Se}$ ; (2) the enough void space among  $\text{M}_{0.85}\text{Se}$  nanosheets allows the redox ions easier diffusion; (3) the two-dimensional morphology provides the large contact area between the CE catalytic material and electrolyte; (4) *in situ* direct growth of the  $\text{M}_{0.85}\text{Se}$  on metal fiber renders the good electrical contact between the active material and the electrons collector.

## Results and discussion

X-ray diffraction (XRD) patterns show the growing nickel selenium and cobalt selenium on the metal fiber could be well indexed to hexagonal  $\text{Ni}_{0.85}\text{Se}$  (JCPDS No. 18-0888) and

<sup>a</sup> National Laboratory of Solid State Microstructures, Collaborative Innovation Center of Advanced Microstructures, Eco-Materials and Renewable Energy Research Center (ERERC), School of Physics, Nanjing University, Nanjing 210093, P.R. China.

<sup>b</sup> School of Chemistry and Chemical Engineering, Nanjing University, Nanjing 210093, P.R. China.

<sup>c</sup> Jiangsu Key Laboratory for Nano Technology, Nanjing University, Nanjing 210093, P.R. China.

<sup>d</sup> College of Chemistry and Pharmaceutical Sciences, Qingdao Agricultural University, Qingdao 266109, P.R. China.

<sup>†</sup> Liang Cheng and Hexing Yin contributed equally to this work.

\*E-mail: [zhouyong1999@nju.edu.cn](mailto:zhouyong1999@nju.edu.cn); [zgou@nju.edu.cn](mailto:zgou@nju.edu.cn)

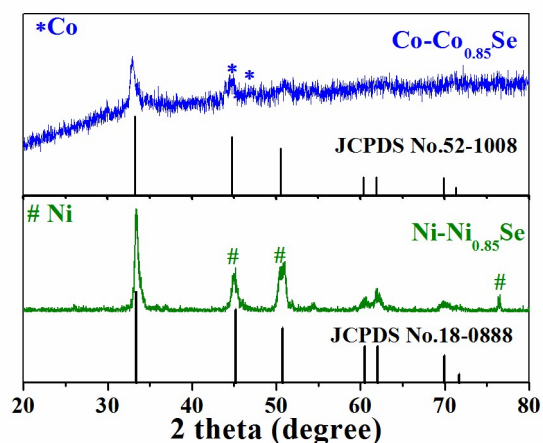


**Fig. 1.** XRD of  $M\text{-}M_{0.85}\text{Se}$ . # is for Ni substrate and \* is for Co substrate.

hexagonal  $\text{Co}_{0.85}\text{Se}$  (JCPDS No. 52-1008), respectively (Fig. 1). The field-emission scanning electron microscopy (FE-SEM) images clearly display that the  $\text{Ni}_{0.85}\text{Se}$  nanosheets were uniformly *in situ* grown on and fully covered the underlying Ni fiber (Fig. 2b and 2c). The high-resolution FE-SEM image further shows that the formed  $\text{Ni}_{0.85}\text{Se}$  nanosheets are about tens of nm in thickness and 1  $\mu\text{m}$  in width, and nearly vertically stand on the fiber substrate (Fig. 2d and 2e). Particularly, the nanosheets were observed to cross-link together to form porous architecture with pore size ranging from 200 to 500 nm, as marked in Fig. 2d. Similarly, the generated  $\text{Co}_{0.85}\text{Se}$  also exhibits nanosheet-like morphology with random arrangement, assembling into a foam-like structure with pore size hundreds of nm (Fig. 2g-2i). The transmission electron microscopy (TEM) images further reveal the two-dimensional morphology of  $\text{Ni}_{0.85}\text{Se}$  and  $\text{Co}_{0.85}\text{Se}$  (Fig. 3a and 3d). The order dot patterns of selected area electron diffraction demonstrate (SAED) that both the  $\text{Ni}_{0.85}\text{Se}$  and  $\text{Co}_{0.85}\text{Se}$  nanosheets are single crystals (Fig. 3c and 3f), implying the potential good electrocatalytic property due to less defects in single-crystal materials. In addition, the TEM image also shows

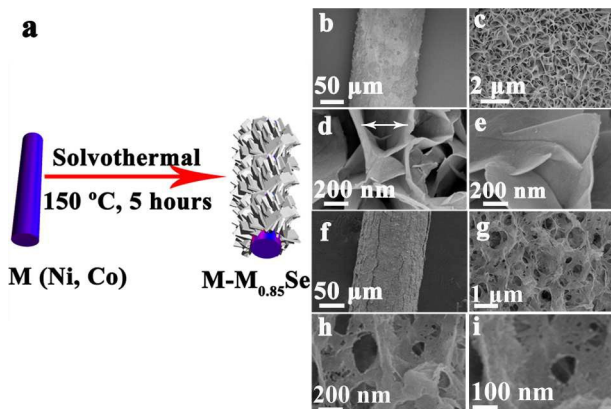


**Fig. 2.** (a) schematic diagram of preparation procedure, (b), (c), (d) and (e) FE-SEM images at different magnifications for  $\text{Ni-Ni}_{0.85}\text{Se}$ , (f), (g), (h) and (i) FE-SEM images at different magnifications for  $\text{Co-Co}_{0.85}\text{Se}$ .

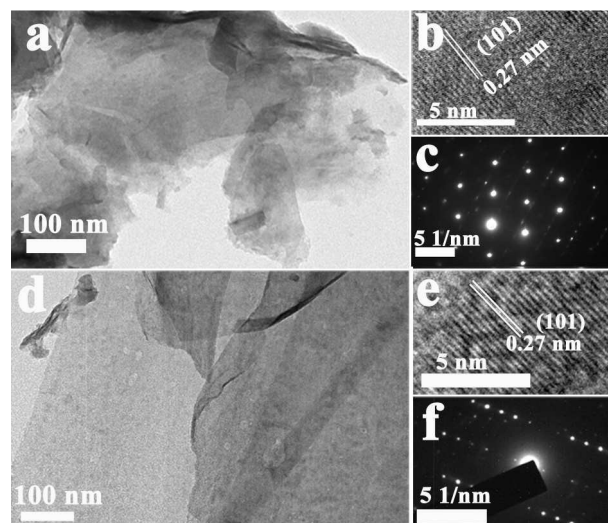


**Fig. 3.** (a) TEM images of  $\text{Ni}_{0.85}\text{Se}$  nanosheets, (b) HRTEM images recorded from  $\text{Ni}_{0.85}\text{Se}$ , (c) SAED images recorded from  $\text{Ni}_{0.85}\text{Se}$ ; (d) TEM images of  $\text{Co}_{0.85}\text{Se}$  nanosheets, (e) HRTEM images recorded from  $\text{Co}_{0.85}\text{Se}$ , (f) SAED images recorded from  $\text{Co}_{0.85}\text{Se}$ .

the ultrathin feature of the  $\text{Co}_{0.85}\text{Se}$  nanosheets with the thickness smaller than 10 nm (Fig. 3d).

The FDSSCs devices were fabricated with the various CEs of similar cell configuration (the preparation process details are showed in supporting information), schematically illustrated in Fig. 4a. The  $M\text{-}M_{0.85}\text{Se}$  or Pt fiber was twisted with the  $\text{TiO}_2$  nanotube array-coated Ti fiber (Fig. S1) as photoanodes, which was then inserted into a transparent capillary filled with electrolyte to be assembled into a FDSSC. The FDSSCs with the  $M\text{-}M_{0.85}\text{Se}$  fibers CEs achieved the power conversion efficiency of 7.07% ( $\text{Ni-Ni}_{0.85}\text{Se}$ ) and 6.55% ( $\text{Co-Co}_{0.85}\text{Se}$ ), respectively, comparable or even superior to that of Pt fiber CE (6.54%) (Fig. 4b and Table 1). The slight higher power conversion efficiency of the  $\text{Ni-Ni}_{0.85}\text{Se}$  arises from higher photocurrent density ( $J_{\text{SC}}$ ).

To further reveal the high performance of the  $M_{0.85}\text{Se}$  nanosheets, the catalytic activity of the  $M\text{-}M_{0.85}\text{Se}$  fibers was conducted with cyclic voltammetry (CV) measurements in three-electrode system. The details of testing were described in Supporting Information. Two pairs of oxidation and reduction peaks in CV curves were observed, which are consistent with as-referred Pt fiber electrode (Fig. 5). In the CV curves, the pair of redox peaks at low potential correspond to the  $\text{I}_3^-/\text{I}^-$  redox reactions, while the pair of redox peaks at high potential can be attributed to  $\text{I}_3^-/\text{I}_2$  redox reactions<sup>14b, 23</sup>. The electrocatalytic activity of the CE can be evaluated from the two parameters of the CV curve, i.e. the peak-to-peak separation ( $\Delta E_p$ ) and the peak current density, and the characteristics of low potential pair peaks separation are generally considered extremely important in analyzing the catalytic activity of CEs in DSSCs. Both  $\Delta E_p$  of the  $\text{Ni-Ni}_{0.85}\text{Se}$  and  $\text{Co-Co}_{0.85}\text{Se}$  are lower than that of Pt fiber (Fig. 5), implying that the charge transfer rate ( $k_s$ ) of both  $M\text{-}M_{0.85}\text{Se}$  fibers electrodes are higher than that of Pt fiber electrode as the  $\Delta E_p$  varies inversely with  $k_s$ <sup>14b</sup>. The  $\text{Ni-Ni}_{0.85}\text{Se}$  electrode exhibits

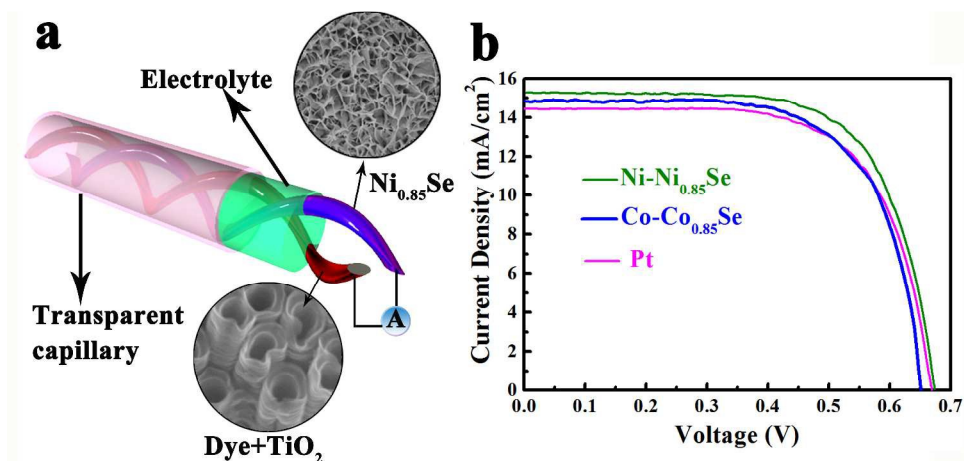


Fig. 4 (a) Schematic setup of the FDSSC, (b) I-V curves of FDSSCs based on Ni-Ni<sub>0.85</sub>Se, Co-Co<sub>0.85</sub>Se and Pt fibers as counter electrodes

**Table 1.** The parameters of various FDSSCs, and the EIS data of various electrodes.

Counter Electrodes	$V_{oc}$ (V)	$J_{sc}$ (mA/cm <sup>2</sup> )	Fill Fact (%)	$\eta$ (%)	$R_s$ ( $\Omega \cdot \text{cm}^2$ )	$R_{ct}$ ( $\Omega \cdot \text{cm}^2$ )	$Z_N$ ( $\Omega \cdot \text{cm}^2$ )
Pt	0.67	14.35	68.41	6.54	1.96	1.04	6.05
Co-Co <sub>0.85</sub> Se	0.65	14.73	68.12	6.55	2.06	0.65	7.53
Ni-Ni <sub>0.85</sub> Se	0.68	15.28	68.05	7.07	2.08	0.38	7.28

higher redox peak current density than Pt and Co-Co<sub>0.85</sub>Se fiber, which may be contributed to the higher power conversion

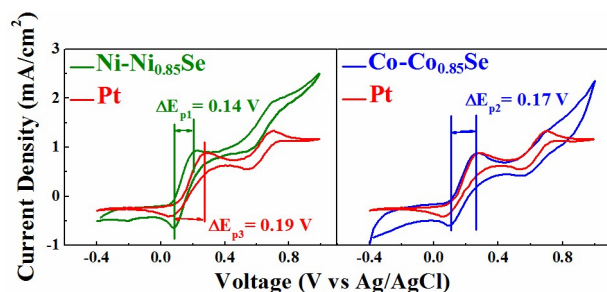


Fig. 5. CV curves for Ni-Ni<sub>0.85</sub>Se, Co-Co<sub>0.85</sub>Se and Pt fibers.

efficiency.

Electrochemical impedance spectroscopy (EIS) experiments were also carried out through using symmetric cells with two identical electrodes (CE/electrolyte/CE) under dark conditions. Fig. 6 shows the Nyquist plots of M-M<sub>0.85</sub>Se fibers and Pt fiber electrodes, respectively. The first arc arises from the charge-transfer resistance ( $R_{ct}$ ) at the CE/electrolyte interface, and the second arc relates to the Nernstian diffusion element ( $Z_N$ )<sup>14b</sup>. The series resistance ( $R_s$ ) corresponds to the intercept of the first

arc on the real axis.  $R_s$  of Ni-Ni<sub>0.85</sub>Se, Co-Co<sub>0.85</sub>Se, and Pt fibers electrodes were measured 2.08  $\Omega \cdot \text{cm}^2$ , 2.06  $\Omega \cdot \text{cm}^2$ , and 1.96  $\Omega \cdot \text{cm}^2$ , respectively.  $R_{ct}$  of the three electrodes were in sequence of Ni-Ni<sub>0.85</sub>Se (0.38  $\Omega \cdot \text{cm}^2$ ) < Co-Co<sub>x</sub>Se (0.65  $\Omega \cdot \text{cm}^2$ ) < Pt (1.04  $\Omega \cdot \text{cm}^2$ ). The smaller  $R_{ct}$  of the Ni-Ni<sub>0.85</sub>Se fiber proves that the Ni<sub>0.85</sub>Se nanosheets exhibit better catalytic activity on the reduction of I<sub>3</sub><sup>-</sup> ions than Pt fiber and Co<sub>0.85</sub>Se, which is consistent with the conclusion obtained from the analysis of CV.

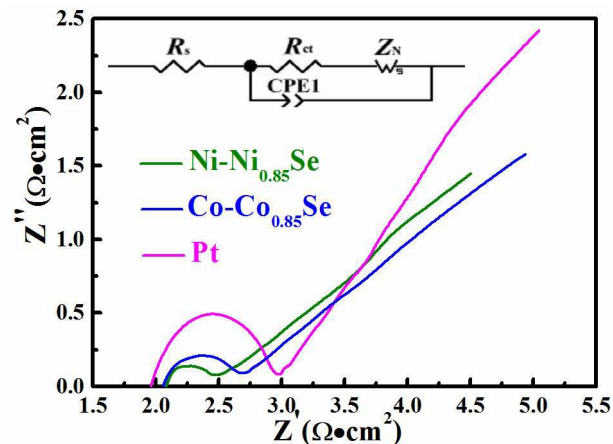


Fig. 6. Nyquist plots of the symmetric cells with two identical counter electrodes of Ni-Ni<sub>0.85</sub>Se, Co-Co<sub>0.85</sub>Se and Pt fibers.

The larger  $Z_N$  of M- $M_{0.85}Se$  fibers originate from the  $M_{0.85}Se$  layers with several  $\mu m$  thickness, which increases the resistance of  $I_3^-/I^-$  ion diffusion.

## Conclusion

The unique  $Ni_{0.85}Se$  and  $Co_{0.85}Se$  nanosheets were successfully *in situ* grown on the metal (Ni or Co) fiber through one-step solvothermal reaction. Both Ni- $Ni_{0.85}Se$  fiber and Co- $Co_{0.85}Se$  fiber exhibit excellent electrochemical catalytic activity for the reduction of  $I_3^-$  to  $I^-$  in FDSSCs. The intrinsic electrocatalytic property, porous architectures, the two-dimensional morphology, and single crystal feature of  $M_{0.85}Se$  were believed to account for the excellent photovoltaic performance of the corresponding FDSSCs. This work has tremendous implications that substitution of a low-cost, easily handled M- $M_{0.85}Se$  fibers CEs with good performance for the precious metal Pt will foster the development of FDSSCs and reduce the cost for energy conversion.

## Acknowledgements

This work was supported by 973 Programs (Nos. 2014CB239302, 2011CB933303, and 2013CB632404), National Science Foundation of Jiangsu Province (Nos. BK2012015 and BK20130053), National Natural Science Foundation of China (Nos. 2147309, 51272101, 51202005).

## Notes and references

- (a) M.R. Lee, R.D. Eckert, K. Forberich, G. Dennler, C.J. Brabec, R.A. Gaudiana, *Science* 2009, **234**, 232; (b) L.B. Qiu, J. Deng, X. Lu, Z.B. Yang, and H.S. Peng, *Angew. Chem. Int. Ed.* 2014, **53**, 10425; (c) B.J. Kim, D.H. Kim, Y.Y. Lee, H.W. Shin, G.S. Han, J.S. Hong, K. Mahmood, T.K. Ahn, Y.C. Joo, K.S. Hong, N.G. Park, S.W. Lee, H.S. Jung, *Energy Environ. Sci.* 2015, **8**, 916; (d) A. Chirilă, S. Buecheler, F. Pianezzi, P. Bloesch, C. Gretener, A.R. Uhl, C. Fella, L. Kranz, J. Perrenoud, S. Seyrling, R. Verma, S. Nishiwaki, Y.E. Romanyuk, G. Bilger, A.N. Tiwari, *Nat. Mater.* 2011, **10**, 857.
- (a) Z.T. Zhang, J. Deng, X.Y. Li, Z.B. Yang, S.S. He, X.L. Chen, G.Z. Guan, J. Ren, and H.S. Peng, *Adv. Mater.* 2015, **27**, 356; (b) Z.B. Yang, J. Deng, H. Sun, J. Ren, S.W. Pan, and H.S. Peng, *Adv. Mater.* 2014, **26**, 7038; (c) Q.F. Wang, X.F. Wang, J. Xu, X. Ouyang, X.J. Hou, D. Chen, R.M. Wang, G.Z. Shen, *Nano Energy* 2014, **8**, 44.
- J.W. Zhong, Y. Zhang, Q.Z. Zhong, Q.Y. Hu, B. Hu, Z.L. Wang, J. Zhou, *ACS Nano* 2014, **8**, 6273.
- (a) Z.B. Yang, J. Deng, X.M. Sun, H.P. Li, and H.S. Peng, *Adv. Mater.* 2014, **26**, 2643; (b) S.W. Pan, Z.B. Yang, P.N. Chen, J. Deng, H.P. Li, and H.S. Peng, *Angew. Chem. Int. Ed.* 2014, **53**, 6110; (c) Z.T. Zhang, X.Y. Li, G.Z. Guan, S.W. Pan, Z.J. Zhu, D.Y. Ren, and H.S. Peng, *Angew. Chem. Int. Ed.* 2014, **53**, 11571.
- (a) D. C. Zou, D. Wang, Z. Z. Chu, Z. B. Lv, X. Fan, *Coord. Chem. Rev.* 2010, **254**, 1169 (b) X. Fan, Z. Chu, F. Wang, C. Zhang, L. Chen, Y. Tang, D. C. Zou, *Adv. Mater.* 2008, **20**, 592; (c) Z. B. Lv, J. F. Yu, H. W. Wu, J. Shang, D. Wang, S. C. Hou, Y. P. Fu, K. Wu, D. C. Zou, *Nanoscale* 2012, **4**, 1248; (d) Y. P. Fu, M. Peng, Z. B. Lv, X. Cai, S. C. Hou, H. W. Wu, X. Yu, H. Kafafy, D. C. Zou, *Nano Energy* 2013, **2**, 537; (e) G.C. Liu, M. Peng, W.X. Song, H. Wang, D.C. Zou, *Nano Energy* 2015, **11**, 341.
- (a) T. Chen, L. B. Qiu, Z. B. Yang, H. S. Peng, *Chem. Soc. Rev.* 2013, **42**, 5031; (b) T. Chen, S. T. Wang, Z. B. Yang, Q. Y. Feng, X. M. Sun, L. Li, Z. S. Wang, H. S. Peng, *Angew. Chem. Int. Ed.* 2011, **50**, 1815; (c) T. Chen, L. B. Qiu, Z. B. Yang, Z. B. Cai, J. Ren, H. P. Li, H. J. Lin, X. M. Sun, H. S. Peng, *Angew. Chem. Int. Ed.* 2012, **51**, 11977; (d) H. Sun, Z. B. Yang, X. L. Chen, L. B. Qiu, X. You, P. H. Chen, H. S. Peng, *Angew. Chem. Int. Ed.* 2013, **52**, 8276; (e) S. W. Pan, Z. B. Yang, H. P. Li, L. B. Qiu, H. Sun, H. S. Peng, *J. Am. Chem. Soc.* 2013, **135**, 10622.
- (a) B. Weintraub, Y. Wei, Z.L. Wang, *Angew. Chem. Int. Ed.* 2009, **48**, 8981; (b) W. X. Guo, C. Xu, X. Wang, S. H. Wang, C. F. Pan, C. J. Lin, Z. L. Wang, *J. Am. Chem. Soc.* 2012, **134**, 4437.
- S. C. Hou, X. Cai, Y. P. Fu, Z. B. Lv, D. Wang, H. W. Wu, C. Zhang, Z. Z. Chu, D. C. Zou, *J. Mater. Chem.* 2011, **21**, 13776.
- S. Zhang, C.Y. Ji, Z.Q. Bian, P.R. Yu, L.H. Zhang, D.Y. Liu, E.Z. Shi, Y.Y. Shang, H.T. Peng, Q. Cheng, D. Wang, C.H. Huang, A.Y. Cao, *ACS Nano* 2012, **6**, 7191.
- Z. B. Yang, H. Sun, T. Chen, L. B. Qiu, Y.F. Luo, H.S. Peng, *Angew. Chem. Int. Ed.* 2013, **52**, 7545.
- T. Chen, L.B. Qiu, Z.B. Cai, F. Gong, Z.B. Yang, Z.S. Wang, and H.S. Peng, *Nano Lett.* 2012, **12**, 2568.
- H. Sun, Z.B. Yang, X.L. Chen, L.B. Qiu, X. You, P.N. Chen, H.S. Peng, *Angew. Chem. Int. Ed.* 2013, **52**, 8276.
- S.C. Hou, X. Cai, H.W. Wu, X. Yu, M. Peng, K. Yan, D.C. Zou, *Energy Environ. Sci.* 2013, **6**, 3356.
- (a) S.N. Yun, A. Hagfeldt, T.L. Ma, *Adv. Mater.* 2014, **26**, 6210; (b) M.X. Wu, X. Lin, Y.D. Wang, L. Wang, W. Guo, D.D. Qi, X.J. Peng, A. Hagfeldt, M. Grätzel, T.L. Ma, *J. Am. Chem. Soc.* 2012, **134**, 3419.
- L. Chen, H. Dai, Y. Zhou, Y.J. Hu, T. Yu, J.G. Liu, Z.G. Zou, *Chem. Commun.* 2014, **50**, 14321.
- M.K. Wang, A.M. Anghel, B. Marsan, N. C. Ha, N. Pootrakulchote, S.M. Zakeeruddin, M. Grätzel, *J. Am. Chem. Soc.* 2009, **131**, 15976.
- S.H. Chang, M.D. Lu, Y.L. Tung, H.Y. Tuan, *ACS Nano*. 2013, **7**, 9443.
- F. Gong, X. Xu, Z.Q. Li, G. Zhou, Z.S. Wang, *Chem. Commun.* 2013, **49**, 1437.
- X.J. Zheng, J.H. Guo, Y.T. Shi, F.Q. Xiong, W.H. Zhang, T.L. Ma and Can Li, *Chem. Commun.* 2013, **49**, 9645.
- L.X. Yi, Y.Y. Liu, N.L. Yang, Z.Y. Tang, H.J. Zhao, G.H. Ma, Z.G. Su, D. Wang, *Energy Environ. Sci.* 2013, **6**, 835.
- C.T. Lee, J.D. Peng, C.T. Li, Y.L. Tsai, R. Vittal, K.C. Ho, *Nano Energy* 2014, **10**, 201.
- C.W. Kung, H.W. Chen, C.Y. Lin, K.C. Huang, R. Vittal, K.C. Ho, *ACS Nano* 2012, **6**, 7016.
- F. Gong, H. Wang, X. Xu, G. Zhou, Z.S. Wang, *J. Am. Chem. Soc.* 2012, **134**, 10953.
- L. Chen, Y. Zhou, H. Dai, T. Yu, J.G. Liu, Z.G. Zou, *Nano Energy* 2015, **11**, 697.

# **Metal (Co, Ni) Selenium Nanosheets on Metal Fibers as Counter Electrodes toward Low-cost, High-Performance Fiber-shaped Dye-sensitized Solar Cells**

Liang Chen, Hexing Yin, Yong Zhou, Hui Dai, Tao Yu, Jianguo Liu and Zhigang Zou

## Supporting Information

### 1 Experimental Section

#### (1) Fabrication of Ni<sub>0.85</sub>Se and Co<sub>0.85</sub>Se nanosheets

0.2 g of metal (Ni, Co) fiber (127  $\mu\text{m}$  diameter) was ultrasonically cleaned with 10 wt% nitric acid aqueous solution several minutes and then in ethanol for 30 min. 0.2 g Se powder and 15 mL of hydrazine hydrate were added into a stainless Teflon-lined autoclave of 50 mL inner volume and stirred for 30 min. The cleaned metal (Ni, Co) fiber was soaked in the solution. The sealed autoclave would be placed into an electric oven at 150°C for 5 h. After synthesis, the sealed autoclaves cool down to room temperature, naturally. The as-prepared fiber was taken out, washed with de-ionized water and ethanol several times.

#### (2) Solar cells fabrication

TiO<sub>2</sub> nanotube grew on Ti fiber (diameter of 250  $\mu\text{m}$ ) which was treated by electrochemical anodization in ethylene glycol mixed with NH<sub>4</sub>F (0.2 wt%) and H<sub>2</sub>O (1 wt%). This anodization was performed under constant voltage 60 V and temperature 25 °C for 7~8 h in a two-electrode system. The anode and cathode electrodes are Ti fiber and carbon rod, respectively. TiO<sub>2</sub> nanotube was obtained through annealing the anodized Ti fiber at 450 °C in air for 2 h (Figure S1). The resulting Ti fiber was heated at 70 °C in 0.2M TiCl<sub>4</sub> solution for 30 min. Following, it was sintered at 450 °C in air for 30 min. After that, the obtained Ti fiber cooled were soaked in 0.5 mM N719 dye solution (solvent mixture of acetonitrile and tert-butyl alcohol in volume ratio of 1:1) and kept for 24~48h at room temperature. Herein, the redox electrolyte is consist of 1.0 M 1-Butyl-3-methylimidazolium iodide (BMIMI), 50 mM LiI, 30 mM I<sub>2</sub> and 0.5 M tert-butylpyridine in a mixed solvent of acetonitrile and 85 valeronitrile (v/v, 85:15). Finally, the dye-sensitized Ti fiber coated with TiO<sub>2</sub> naotube and counter electrode (Ni-Ni<sub>0.85</sub>Se, Co-Co<sub>0.85</sub>Se or Pt fiber) were inserted into a transparent

capillary filled with electrolyte in order to assemble into a fiber-shaped dye-sensitized solar cell (FDSSC). The effective active area of the cell is calculated by multiplying the diameter (0.03 cm) of photoanode and effective length (3 cm) of the cell. The active area of FDSSCs is about 0.09 cm<sup>2</sup>.

## 2 Characterization

Field-emission scanning electron microscopy (FE-SEM) images were obtained on an S-4800 scanning electron microscopy operating at 5 kV. The transmission electron microscopy (TEM), High-resolution transmission electron microscopy (HRTEM) and selected area electron diffraction (SAED) images were observed on a JEM 200CX TEM instrument. The crystallographic phase of the as-prepared products was determined by powder X-ray diffraction (XRD) (Rigaku Ultima III, Japan) using Cu-K $\alpha$  radiation ( $\lambda=0.154178$  nm) with scan rate of 100 min<sup>-1</sup> at 40 kV and 40 mA. Photocurrent-Voltage (I-V) measurements were carried out, with the length FDSSC of 3 cm, on a Keithley 236 source measurement unit under AM 1.5 illumination cast by an Oriel 92251A-1000 sunlight simulator calibrated by the standard reference of a Newport 91150 silicon solar cell. Electrochemical impedance spectroscopic (EIS) curves of the symmetric cells fabricated with two identical electrodes (CE/electrolyte/CE) were observed by PAR2273 workstation (Princeton Applied Research, USA) with a 10 mV amplitude perturbation and the frequency range was from 100 mHz to 100 kHz. The cyclic voltammetry measurements (CV) are conducted in a three-electrode system at a scan rate of 50 mV•S<sup>-1</sup> by using PAR2273 workstation (Princeton Applied Research, USA). The counter and reference electrode are Pt and Ag/AgCl composite electrode, respectively. In CV testing, the I<sub>3</sub><sup>-</sup>/I<sup>-</sup> electrolyte contained 0.1 M LiClO<sub>4</sub>, 10 mM LiI, and 1 mM I<sub>2</sub> in acetonitrile.

## 3 Figure

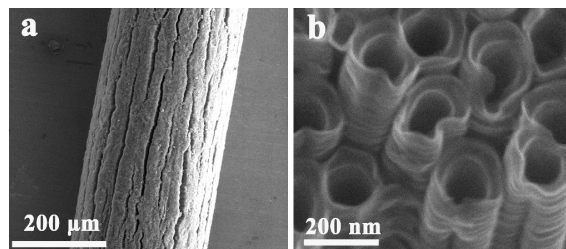


**Figure S1.** a) FE-SEM images of Ti fiber coating with TiO<sub>2</sub> nanotube, b) high magnification FE-SEM images of TiO<sub>2</sub> nanotube.

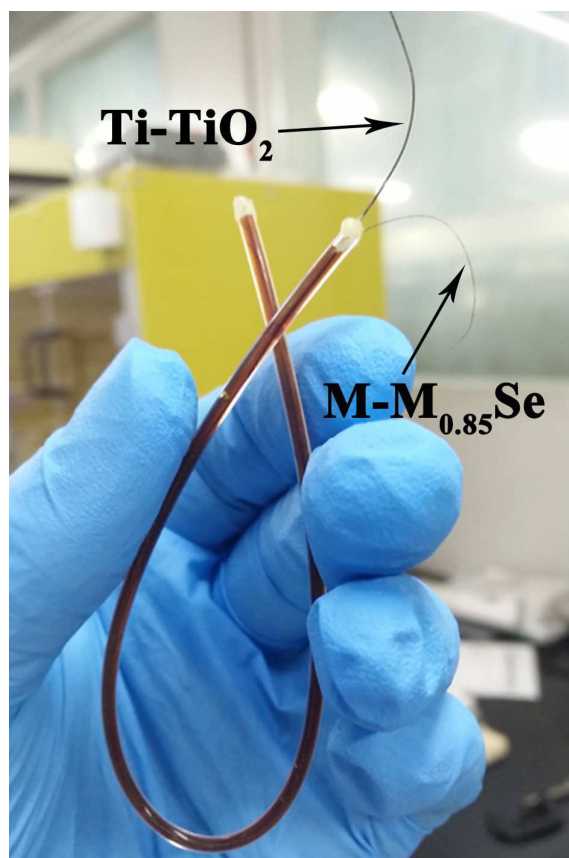
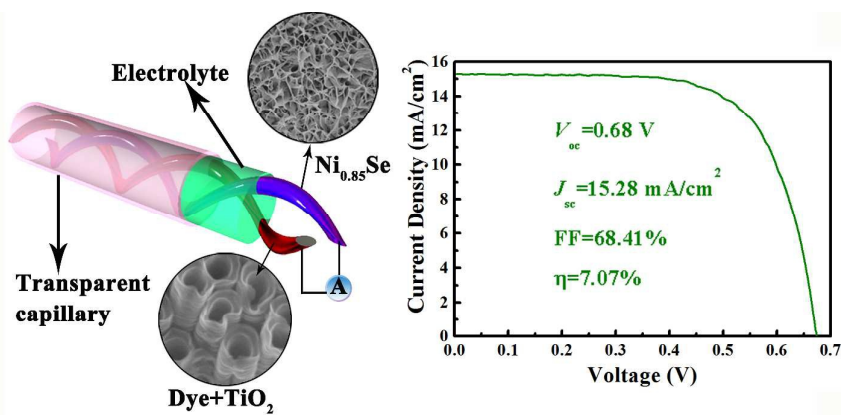


**Figure S2.** Photograph of FDSSC based on the Ni<sub>0.85</sub>Se CE.



# *In Situ* Direct Growth of Single Crystalline Metal (Co, Ni) Selenium Nanosheets on Metal Fibers as Counter Electrodes toward Low-cost, High-Performance Fiber-shaped Dye-sensitized Solar Cells

Liang Chen<sup>†a</sup>, Hexing Yin<sup>†b</sup>, Yong Zhou<sup>a,c\*</sup>, Hui Dai<sup>a,d</sup>, Tao Yu<sup>a,c</sup>, Jianguo Liu<sup>a,c</sup> and Zhigang Zou<sup>a,c\*</sup>

Received (in XXX, XXX) Xth XXXXXXXXX 200X, Accepted Xth XXXXXXXXX 200X

First published on the web Xth XXXXXXXXX 200X

DOI: 10.1039/b000000x

Highly crystalline metal (Co, Ni) selenium ( $\text{Co}_{0.85}\text{Se}$  or  $\text{Ni}_{0.85}\text{Se}$ ) nanosheets were *in situ* grown on metal (Co, Ni) fibers ( $\text{M-M}_{0.85}\text{Se}$ ). Both  $\text{M-M}_{0.85}\text{Se}$  ( $\text{Co-Co}_{0.85}\text{Se}$  and  $\text{Ni-Ni}_{0.85}\text{Se}$ ) fibers prove to function as excellent, low-cost counter electrodes (CEs) in fiber-shaped dye-sensitized solar cells (FDSSCs) with high power conversion efficiency ( $\text{Co-Co}_{0.85}\text{Se}$  6.55% and  $\text{Ni-Ni}_{0.85}\text{Se}$  7.07%), comparable or even superior to Pt fiber CE (6.54%). The good performance of the present Pt-free CE-based solar cell was believed to originate from: (1) the intrinsic electrocatalytic property of the single-crystalline  $\text{M-M}_{0.85}\text{Se}$ ; (2) the enough void space among  $\text{M}_{0.85}\text{Se}$  nanosheets allows the redox ions easier diffusion; (3) the two-dimensional morphology provides the large contact area between the CE catalytic material and electrolyte; (4) *in situ* direct growth of the  $\text{M}_{0.85}\text{Se}$  on metal fiber renders the good electrical contact between the active material and the electrons collector.

## Introduction

As portable electric devices become more and more popularity, wearable devices (solar cells<sup>1</sup>, supercapacitors<sup>2</sup>, and generators<sup>3</sup>) have been rapidly attracting attentions. Fiber-shaped solar cells can be woven into wearable energy cloths (such as coats, hats or bags) to charge portable electric devices in a very handy way<sup>4</sup>. Currently, fiber-shaped dye-sensitized solar cells (FDSSCs), in sharp contrast with the flat counterpart, represent typical fiber-configuration electronics for solar energy harvesting<sup>5-13</sup>. A typical FDSSC consists of a fiber-shaped photoanode (n-type semiconductor film sensitized with dye), a redox electrolyte (an organic liquid solvent dissolving with  $\text{I}_3^-/\text{I}^-$  redox species), and a fiber-shaped counter electrode (CE).

Optimization of the  $\text{I}_3^-$  reduction reaction conducted with CE is of utmost significance for enhancement of photovoltaic performance of a FDSSC. Pt fiber proves to be a well stable and high efficient electrocatalyst in liquid state FDSSCs for  $\text{I}_3^-/\text{I}^-$  redox couple. Motivated by practical and economical considerations, great effort was made to explore low-cost, Pt-free

CE, such as specific transition metal carbides<sup>14</sup>, nitrides<sup>14,15</sup> and chalcogens<sup>16-24</sup>. The Pt-free CE used for the FDSSC generally grows on a tread-like conductive substrate that collects electrons from the external load and transfers electrons into the electrocatalyst film<sup>13-24</sup>. The good performance of the Pt-free CE could be achieved through mediating the feature of the CE, including improving surface area, enhancing electrical conductivity, or exposing high-activity crystal facet.

In this paper, we directly grew single-crystalline metal (Ni, Co) selenium nanosheets on metal fiber (briefly called as  $\text{M-M}_{0.85}\text{Se}$ ) toward low-cost, high-performance FDSSCs. The growing  $\text{M}_{0.85}\text{Se}$  nanosheets layer acts as electrocatalytic centers for the reduction of  $\text{I}_3^-$ , and the underlying metal fiber as conductive collector for collecting electrons. Photovoltaic measurement demonstrates that the  $\text{M-M}_{0.85}\text{Se}$  thus obtained show good electrocatalytic behavior as CEs for the high-efficiency FDSSC ( $\text{Ni-Ni}_{0.85}\text{Se}$  for 7.07% and  $\text{Co-Co}_{0.85}\text{Se}$  for 6.55%), comparable or even superior to Pt fiber (6.54%). The good performance of the present Pt-free CE-based solar cell was believed to originate from: (1) the intrinsic electrocatalytic property of the single-crystalline  $\text{M-M}_{0.85}\text{Se}$ ; (2) the enough void space among  $\text{M}_{0.85}\text{Se}$  nanosheets allows the redox ions easier diffusion; (3) the two-dimensional morphology provides the large contact area between the CE catalytic material and electrolyte; (4) *in situ* direct growth of the  $\text{M}_{0.85}\text{Se}$  on metal fiber renders the good electrical contact between the active material and the electrons collector.

## Results and discussion

X-ray diffraction (XRD) patterns show the growing nickel selenium and cobalt selenium on the metal fiber could be well indexed to hexagonal  $\text{Ni}_{0.85}\text{Se}$  (JCPDS No. 18-0888) and

<sup>a</sup> National Laboratory of Solid State Microstructures, Collaborative Innovation Center of Advanced Microstructures, Eco-Materials and Renewable Energy Research Center (ERERC), School of Physics, Nanjing University, Nanjing 210093, P.R. China.

<sup>b</sup> School of Chemistry and Chemical Engineering, Nanjing University, Nanjing 210093, P.R. China.

<sup>c</sup> Jiangsu Key Laboratory for Nano Technology, Nanjing University, Nanjing 210093, P.R. China.

<sup>d</sup> College of Chemistry and Pharmaceutical Sciences, Qingdao Agricultural University, Qingdao 266109, P.R. China.

<sup>†</sup> Liang Cheng and Hexing Yin contributed equally to this work.

\*E-mail: [zhouyong1999@nju.edu.cn](mailto:zhouyong1999@nju.edu.cn); [zgou@nju.edu.cn](mailto:zgou@nju.edu.cn)

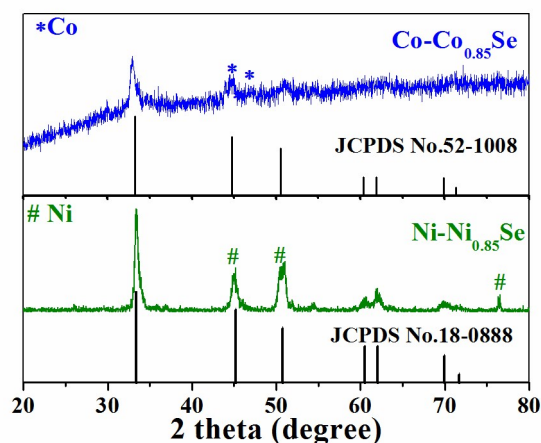


**Fig. 1.** XRD of M- $M_{0.85}\text{Se}$ . # is for Ni substrate and \* is for Co substrate.

hexagonal  $\text{Co}_{0.85}\text{Se}$  (JCPDS No. 52-1008), respectively (Fig. 1). The field-emission scanning electron microscopy (FE-SEM) images clearly display that the  $\text{Ni}_{0.85}\text{Se}$  nanosheets were uniformly *in situ* grown on and fully covered the underlying Ni fiber (Fig. 2b and 2c). The high-resolution FE-SEM image further shows that the formed  $\text{Ni}_{0.85}\text{Se}$  nanosheets are about tens of nm in thickness and 1  $\mu\text{m}$  in width, and nearly vertically stand on the fiber substrate (Fig. 2d and 2e). Particularly, the nanosheets were observed to cross-link together to form porous architecture with pore size ranging from 200 to 500 nm, as marked in Fig. 2d. Similarly, the generated  $\text{Co}_{0.85}\text{Se}$  also exhibits nanosheet-like morphology with random arrangement, assembling into a foam-like structure with pore size hundreds of nm (Fig. 2g-2i). The transmission electron microscopy (TEM) images further reveal the two-dimensional morphology of  $\text{Ni}_{0.85}\text{Se}$  and  $\text{Co}_{0.85}\text{Se}$  (Fig. 3a and 3d). The order dot patterns of selected area electron diffraction demonstrate (SAED) that both the  $\text{Ni}_{0.85}\text{Se}$  and  $\text{Co}_{0.85}\text{Se}$  nanosheets are single crystals (Fig. 3c and 3f), implying the potential good electrocatalytic property due to less defects in single-crystal materials. In addition, the TEM image also shows

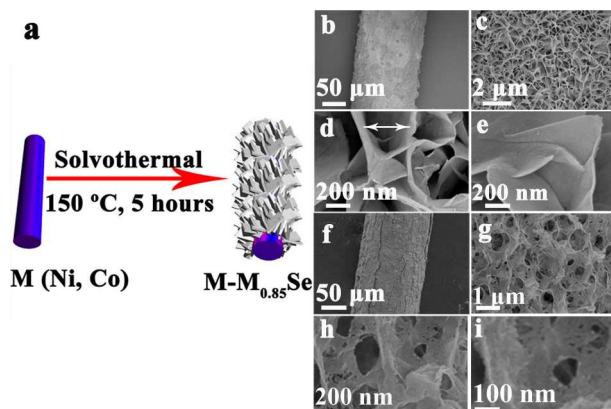


**Fig. 2.** (a) schematic diagram of preparation procedure, (b), (c), (d) and (e) FE-SEM images at different magnifications for  $\text{Ni-Ni}_{0.85}\text{Se}$ , (f), (g), (h) and (i) FE-SEM images at different magnifications for  $\text{Co-Co}_{0.85}\text{Se}$ .

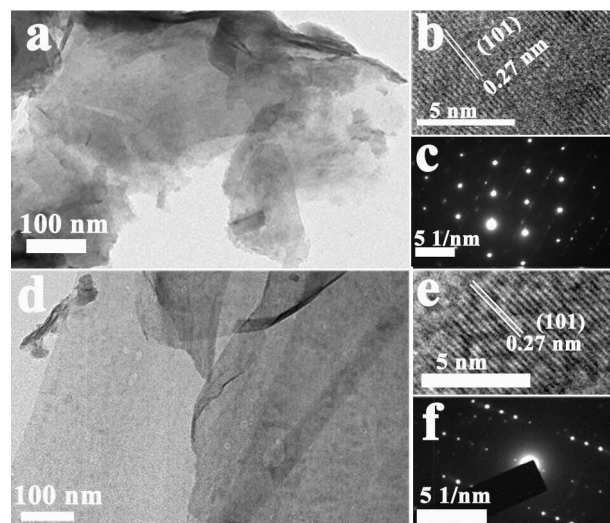


**Fig. 3.** (a) TEM images of  $\text{Ni}_{0.85}\text{Se}$  nanosheets, (b) HRTEM images recorded from  $\text{Ni}_{0.85}\text{Se}$ , (c) SAED images recorded from  $\text{Ni}_{0.85}\text{Se}$ ; (d) TEM images of  $\text{Co}_{0.85}\text{Se}$  nanosheets, (e) HRTEM images recorded from  $\text{Co}_{0.85}\text{Se}$ , (f) SAED images recorded from  $\text{Co}_{0.85}\text{Se}$ .

the ultrathin feature of the  $\text{Co}_{0.85}\text{Se}$  nanosheets with the thickness smaller than 10 nm (Fig. 3d).

The FDSSCs devices were fabricated with the various CEs of similar cell configuration (the preparation process details are showed in supporting information), schematically illustrated in Fig. 4a. The M- $M_{0.85}\text{Se}$  or Pt fiber was twisted with the  $\text{TiO}_2$  nanotube array-coated Ti fiber (Fig. S1) as photoanodes, which was then inserted into a transparent capillary filled with electrolyte to be assembled into a FDSSC. The FDSSCs with the M- $M_{0.85}\text{Se}$  fibers CEs achieved the power conversion efficiency of 7.07% ( $\text{Ni-Ni}_{0.85}\text{Se}$ ) and 6.55% ( $\text{Co-Co}_{0.85}\text{Se}$ ), respectively, comparable or even superior to that of Pt fiber CE (6.54%) (Fig. 4b and Table 1). The slight higher power conversion efficiency of the  $\text{Ni-Ni}_{0.85}\text{Se}$  arises from higher photocurrent density ( $J_{\text{SC}}$ ).

To further reveal the high performance of the  $M_{0.85}\text{Se}$  nanosheets, the catalytic activity of the M- $M_{0.85}\text{Se}$  fibers was conducted with cyclic voltammetry (CV) measurements in three-electrode system. The details of testing were described in Supporting Information. Two pairs of oxidation and reduction peaks in CV curves were observed, which are consistent with as-referred Pt fiber electrode (Fig. 5). In the CV curves, the pair of redox peaks at low potential correspond to the  $\text{I}_3^-/\text{I}^-$  redox reactions, while the pair of redox peaks at high potential can be attributed to  $\text{I}_3^-/\text{I}_2$  redox reactions<sup>14b, 23</sup>. The electrocatalytic activity of the CE can be evaluated from the two parameters of the CV curve, i.e. the peak-to-peak separation ( $\Delta E_p$ ) and the peak current density, and the characteristics of low potential pair peaks separation are generally considered extremely important in analyzing the catalytic activity of CEs in DSSCs. Both  $\Delta E_p$  of the  $\text{Ni-Ni}_{0.85}\text{Se}$  and  $\text{Co-Co}_{0.85}\text{Se}$  are lower than that of Pt fiber (Fig. 5), implying that the charge transfer rate ( $k_s$ ) of both M- $M_{0.85}\text{Se}$  fibers electrodes are higher than that of Pt fiber electrode as the  $\Delta E_p$  varies inversely with  $k_s$ <sup>14b</sup>. The  $\text{Ni-Ni}_{0.85}\text{Se}$  electrode exhibits

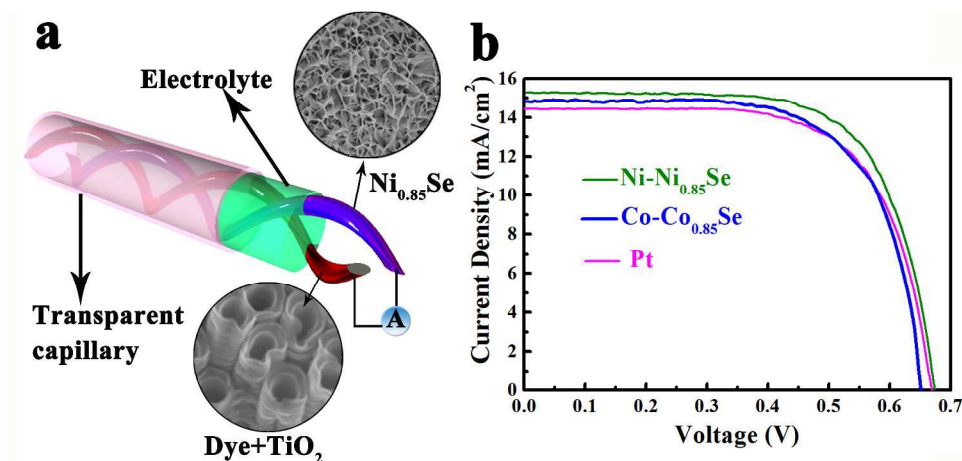


Fig. 4 (a) Schematic setup of the FDSSC, (b) I-V curves of FDSSCs based on Ni-Ni<sub>0.85</sub>Se, Co-Co<sub>0.85</sub>Se and Pt fibers as counter electrodes

**Table 1.** The parameters of various FDSSCs, and the EIS data of various electrodes.

Counter Electrodes	$V_{oc}$ (V)	$J_{sc}$ (mA/cm <sup>2</sup> )	Fill Fact (%)	$\eta$ (%)	$R_s$ ( $\Omega \cdot \text{cm}^2$ )	$R_{ct}$ ( $\Omega \cdot \text{cm}^2$ )	$Z_N$ ( $\Omega \cdot \text{cm}^2$ )
Pt	0.67	14.35	68.41	6.54	1.96	1.04	6.05
Co-Co <sub>0.85</sub> Se	0.65	14.73	68.12	6.55	2.06	0.65	7.53
Ni-Ni <sub>0.85</sub> Se	0.68	15.28	68.05	7.07	2.08	0.38	7.28

higher redox peak current density than Pt and Co-Co<sub>0.85</sub>Se fiber, which may be contributed to the higher power conversion

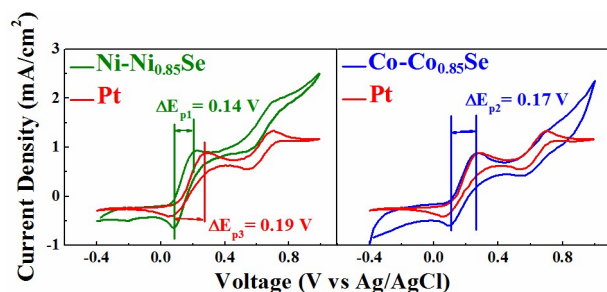


Fig. 5. CV curves for Ni-Ni<sub>0.85</sub>Se, Co-Co<sub>0.85</sub>Se and Pt fibers.

efficiency.

Electrochemical impedance spectroscopy (EIS) experiments were also carried out through using symmetric cells with two identical electrodes (CE/electrolyte/CE) under dark conditions. Fig. 6 shows the Nyquist plots of M-M<sub>0.85</sub>Se fibers and Pt fiber electrodes, respectively. The first arc arises from the charge-transfer resistance ( $R_{ct}$ ) at the CE/electrolyte interface, and the second arc relates to the Nernstian diffusion element ( $Z_N$ )<sup>14b</sup>. The series resistance ( $R_s$ ) corresponds to the intercept of the first

arc on the real axis.  $R_s$  of Ni-Ni<sub>0.85</sub>Se, Co-Co<sub>0.85</sub>Se, and Pt fibers electrodes were measured 2.08  $\Omega \cdot \text{cm}^2$ , 2.06  $\Omega \cdot \text{cm}^2$ , and 1.96  $\Omega \cdot \text{cm}^2$ , respectively.  $R_{ct}$  of the three electrodes were in sequence of Ni-Ni<sub>0.85</sub>Se (0.38  $\Omega \cdot \text{cm}^2$ ) < Co-Co<sub>x</sub>Se (0.65  $\Omega \cdot \text{cm}^2$ ) < Pt (1.04  $\Omega \cdot \text{cm}^2$ ). The smaller  $R_{ct}$  of the Ni-Ni<sub>0.85</sub>Se fiber proves that the Ni<sub>0.85</sub>Se nanosheets exhibit better catalytic activity on the reduction of I<sub>3</sub><sup>-</sup> ions than Pt fiber and Co<sub>0.85</sub>Se, which is consistent with the conclusion obtained from the analysis of CV.

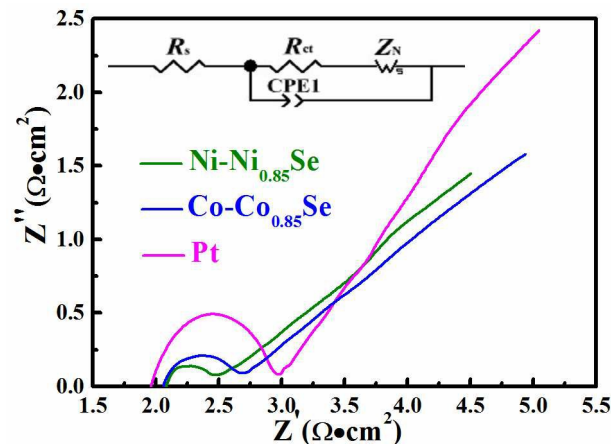


Fig. 6. Nyquist plots of the symmetric cells with two identical counter electrodes of Ni-Ni<sub>0.85</sub>Se, Co-Co<sub>0.85</sub>Se and Pt fibers.

The larger  $Z_N$  of M- $M_{0.85}Se$  fibers originate from the  $M_{0.85}Se$  layers with several  $\mu m$  thickness, which increases the resistance of  $I_3^-/I^-$  ion diffusion.

## Conclusion

The unique  $Ni_{0.85}Se$  and  $Co_{0.85}Se$  nanosheets were successfully *in situ* grown on the metal (Ni or Co) fiber through one-step solvothermal reaction. Both Ni- $Ni_{0.85}Se$  fiber and Co- $Co_{0.85}Se$  fiber exhibit excellent electrochemical catalytic activity for the reduction of  $I_3^-$  to  $I^-$  in FDSSCs. The intrinsic electrocatalytic property, porous architectures, the two-dimensional morphology, and single crystal feature of  $M_{0.85}Se$  were believed to account for the excellent photovoltaic performance of the corresponding FDSSCs. This work has tremendous implications that substitution of a low-cost, easily handled M- $M_{0.85}Se$  fibers CEs with good performance for the precious metal Pt will foster the development of FDSSCs and reduce the cost for energy conversion.

## Acknowledgements

This work was supported by 973 Programs (Nos. 2014CB239302, 2011CB933303, and 2013CB632404), National Science Foundation of Jiangsu Province (Nos. BK2012015 and BK20130053), National Natural Science Foundation of China (Nos. 2147309, 51272101, 51202005).

## Notes and references

- (a) M.R. Lee, R.D. Eckert, K. Forberich, G. Dennler, C.J. Brabec, R.A. Gaudiana, *Science* 2009, **234**, 232; (b) L.B. Qiu, J. Deng, X. Lu, Z.B. Yang, and H.S. Peng, *Angew. Chem. Int. Ed.* 2014, **53**, 10425; (c) B.J. Kim, D.H. Kim, Y.Y. Lee, H.W. Shin, G.S. Han, J.S. Hong, K. Mahmood, T.K. Ahn, Y.C. Joo, K.S. Hong, N.G. Park, S.W. Lee, H.S. Jung, *Energy Environ. Sci.* 2015, **8**, 916; (d) A. Chirilă, S. Buecheler, F. Pianezzi, P. Bloesch, C. Gretener, A.R. Uhl, C. Fella, L. Kranz, J. Perrenoud, S. Seyrling, R. Verma, S. Nishiwaki, Y.E. Romanyuk, G. Bilger, A.N. Tiwari, *Nat. Mater.* 2011, **10**, 857.
- (a) Z.T. Zhang, J. Deng, X.Y. Li, Z.B. Yang, S.S. He, X.L. Chen, G.Z. Guan, J. Ren, and H.S. Peng, *Adv. Mater.* 2015, **27**, 356; (b) Z.B. Yang, J. Deng, H. Sun, J. Ren, S.W. Pan, and H.S. Peng, *Adv. Mater.* 2014, **26**, 7038; (c) Q.F. Wang, X.F. Wang, J. Xu, X. Ouyang, X.J. Hou, D. Chen, R.M. Wang, G.Z. Shen, *Nano Energy* 2014, **8**, 44.
- J.W. Zhong, Y. Zhang, Q.Z. Zhong, Q.Y. Hu, B. Hu, Z.L. Wang, J. Zhou, *ACS Nano* 2014, **8**, 6273.
- (a) Z.B. Yang, J. Deng, X.M. Sun, H.P. Li, and H.S. Peng, *Adv. Mater.* 2014, **26**, 2643; (b) S.W. Pan, Z.B. Yang, P.N. Chen, J. Deng, H.P. Li, and H.S. Peng, *Angew. Chem. Int. Ed.* 2014, **53**, 6110; (c) Z.T. Zhang, X.Y. Li, G.Z. Guan, S.W. Pan, Z.J. Zhu, D.Y. Ren, and H.S. Peng, *Angew. Chem. Int. Ed.* 2014, **53**, 11571.
- (a) D. C. Zou, D. Wang, Z. Z. Chu, Z. B. Lv, X. Fan, *Coord. Chem. Rev.* 2010, **254**, 1169 (b) X. Fan, Z. Chu, F. Wang, C. Zhang, L. Chen, Y. Tang, D. C. Zou, *Adv. Mater.* 2008, **20**, 592; (c) Z. B. Lv, J. F. Yu, H. W. Wu, J. Shang, D. Wang, S. C. Hou, Y. P. Fu, K. Wu, D. C. Zou, *Nanoscale* 2012, **4**, 1248; (d) Y. P. Fu, M. Peng, Z. B. Lv, X. Cai, S. C. Hou, H. W. Wu, X. Yu, H. Kafafy, D. C. Zou, *Nano Energy* 2013, **2**, 537; (e) G.C. Liu, M. Peng, W.X. Song, H. Wang, D.C. Zou, *Nano Energy* 2015, **11**, 341.
- (a) T. Chen, L. B. Qiu, Z. B. Yang, H. S. Peng, *Chem. Soc. Rev.* 2013, **42**, 5031; (b) T. Chen, S. T. Wang, Z. B. Yang, Q. Y. Feng, X. M. Sun, L. Li, Z. S. Wang, H. S. Peng, *Angew. Chem. Int. Ed.* 2011, **50**, 1815; (c) T. Chen, L. B. Qiu, Z. B. Yang, Z. B. Cai, J. Ren, H. P. Li, H. J. Lin, X. M. Sun, H. S. Peng, *Angew. Chem. Int. Ed.* 2012, **51**, 11977; (d) H. Sun, Z. B. Yang, X. L. Chen, L. B. Qiu, X. You, P. H. Chen, H. S. Peng, *Angew. Chem. Int. Ed.* 2013, **52**, 8276; (e) S. W. Pan, Z. B. Yang, H. P. Li, L. B. Qiu, H. Sun, H. S. Peng, *J. Am. Chem. Soc.* 2013, **135**, 10622.
- (a) B. Weintraub, Y. Wei, Z.L. Wang, *Angew. Chem. Int. Ed.* 2009, **48**, 8981; (b) W. X. Guo, C. Xu, X. Wang, S. H. Wang, C. F. Pan, C. J. Lin, Z. L. Wang, *J. Am. Chem. Soc.* 2012, **134**, 4437.
- S. C. Hou, X. Cai, Y. P. Fu, Z. B. Lv, D. Wang, H. W. Wu, C. Zhang, Z. Z. Chu, D. C. Zou, *J. Mater. Chem.* 2011, **21**, 13776.
- S. Zhang, C.Y. Ji, Z.Q. Bian, P.R. Yu, L.H. Zhang, D.Y. Liu, E.Z. Shi, Y.Y. Shang, H.T. Peng, Q. Cheng, D. Wang, C.H. Huang, A.Y. Cao, *ACS Nano* 2012, **6**, 7191.
- Z. B. Yang, H. Sun, T. Chen, L. B. Qiu, Y.F. Luo, H.S. Peng, *Angew. Chem. Int. Ed.* 2013, **52**, 7545.
- T. Chen, L.B. Qiu, Z.B. Cai, F. Gong, Z.B. Yang, Z.S. Wang, and H.S. Peng, *Nano Lett.* 2012, **12**, 2568.
- H. Sun, Z.B. Yang, X.L. Chen, L.B. Qiu, X. You, P.N. Chen, H.S. Peng, *Angew. Chem. Int. Ed.* 2013, **52**, 8276.
- S.C. Hou, X. Cai, H.W. Wu, X. Yu, M. Peng, K. Yan, D.C. Zou, *Energy Environ. Sci.* 2013, **6**, 3356.
- (a) S.N. Yun, A. Hagfeldt, T.L. Ma, *Adv. Mater.* 2014, **26**, 6210; (b) M.X. Wu, X. Lin, Y.D. Wang, L. Wang, W. Guo, D.D. Qi, X.J. Peng, A. Hagfeldt, M. Grätzel, T.L. Ma, *J. Am. Chem. Soc.* 2012, **134**, 3419.
- L. Chen, H. Dai, Y. Zhou, Y.J. Hu, T. Yu, J.G. Liu, Z.G. Zou, *Chem. Commun.* 2014, **50**, 14321.
- M.K. Wang, A.M. Anghel, B. Marsan, N. C. Ha, N. Pootrakulchote, S.M. Zakeeruddin, M. Grätzel, *J. Am. Chem. Soc.* 2009, **131**, 15976.
- S.H. Chang, M.D. Lu, Y.L. Tung, H.Y. Tuan, *ACS Nano*. 2013, **7**, 9443.
- F. Gong, X. Xu, Z.Q. Li, G. Zhou, Z.S. Wang, *Chem. Commun.* 2013, **49**, 1437.
- X.J. Zheng, J.H. Guo, Y.T. Shi, F.Q. Xiong, W.H. Zhang, T.L. Ma and Can Li, *Chem. Commun.* 2013, **49**, 9645.
- L.X. Yi, Y.Y. Liu, N.L. Yang, Z.Y. Tang, H.J. Zhao, G.H. Ma, Z.G. Su, D. Wang, *Energy Environ. Sci.* 2013, **6**, 835.
- C.T. Lee, J.D. Peng, C.T. Li, Y.L. Tsai, R. Vittal, K.C. Ho, *Nano Energy* 2014, **10**, 201.
- C.W. Kung, H.W. Chen, C.Y. Lin, K.C. Huang, R. Vittal, K.C. Ho, *ACS Nano* 2012, **6**, 7016.
- F. Gong, H. Wang, X. Xu, G. Zhou, Z.S. Wang, *J. Am. Chem. Soc.* 2012, **134**, 10953.
- L. Chen, Y. Zhou, H. Dai, T. Yu, J.G. Liu, Z.G. Zou, *Nano Energy* 2015, **11**, 697.